

# Chiral Corrections to Hyperon Axial Form Factors

Fu-Jiun Jiang<sup>1,\*</sup> and B. C. Tiburzi<sup>2,3,†</sup>

<sup>1</sup>*Institute for Theoretical Physics, Bern University,  
Sidlerstrasse 5, CH-3012 Bern, Switzerland*

<sup>2</sup>*Department of Physics, Duke University,  
Box 90305, Durham, NC 27708-0305, USA*

<sup>3</sup>*Maryland Center for Fundamental Physics,  
Department of Physics, University of Maryland,  
College Park, MD 20742-4111, USA*

(Dated: March 17, 2008)

## Abstract

We study the complete set of flavor changing hyperon axial current matrix elements at small momentum transfer. Using partially quenched heavy baryon chiral perturbation theory, we derive the chiral and momentum behavior of the axial and induced pseudoscalar form factors. The meson pole contributions to the latter posses a striking signal for chiral physics. We argue that the study of hyperon axial matrix elements enables a systematic lattice investigation of the efficacy of three flavor chiral expansions in the baryon sector. This can be achieved by considering chiral corrections to  $SU(3)$  symmetry predictions, and their partially quenched generalizations. In particular, despite the presence of eight unknown low-energy constants, we are able to make next-to-leading order symmetry breaking predictions for two linear combinations of axial charges.

PACS numbers: 12.38.Gc, 12.39.Fe

---

\*fjiang@itp.unibe.ch

†bctiburz@umd.edu

## I. INTRODUCTION

For the last decade, lattice gauge theory techniques have made dramatic progress in increasing our understanding of the non-perturbative regime of QCD [1]. Despite considerable advances, there are still sources of systematic error in lattice data, for example, the finite extent of the lattice and the unphysically large quark masses. Fortunately low-energy hadron properties are dominated by virtual pion interactions and the systematic treatment of such interactions using chiral perturbation theory ( $\chi$ PT) allows one to parametrize the lattice volume and quark mass dependence of certain observables. There has been considerable activity to understand theoretically the quark mass and lattice volume dependence of hadronic observables. Further extensions of chiral perturbation theory have been developed to account for quenching and partially quenching [2, 3, 4, 5], and discretization errors [6, 7]. An example is the nucleon axial charge,  $g_A$ . Recent lattice studies have made impressive strides toward determining  $g_A$  [8, 9]. In tandem, recent  $\chi$ PT analyses of the chiral [10, 11, 12], continuum [13, 14] and volume extrapolations [15, 16, 17] are poised to connect the data to the physical point. We are beginning to enter a stage in which the combination of lattice QCD data and  $\chi$ PT will enable the study the hadronic properties from the first principles.

A serious issue, however, confronts this program when extended to hyperon observables. Various  $SU(3)$  predictions for hyperon properties compare poorly to experiment in contrast to the many successful  $SU(2)$  predictions for the nucleon. While  $\chi$ PT can be used to systematically incorporate effects from the strange quark mass, the systematic expansion in the baryon sector has terms that scale (in the worst case) as  $\sim m_\eta/M$ , where  $m_\eta$  is the mass of the  $\eta$ -meson and  $M$  is the average hyperon mass. A well known conflict between  $\chi$ PT analyses and experimental data exist for hyperon decays. For example, the non-leptonic weak decays,  $\Lambda \rightarrow p\pi^-$  and  $\Sigma^+ \rightarrow n\pi^+$ , have been extensively investigated experimentally. In particular the  $s$ - and  $p$ -wave contributions to these weak decays are determined to high precision. Although efforts in the framework of  $\chi$ PT have been devoted to understand these non-leptonic decays theoretically [18, 19, 20, 21, 22, 23, 24, 25, 26, 27], long-standing disagreement between these theoretical analyses and experimental data remain [28, 29, 30].

One is thus led to question the efficacy of three-flavor  $\chi$ PT in the baryon sector. Without this systematic model-independent expansion, lattice QCD data for hyperon properties cannot be reliably extrapolated to the physical values of the quark masses. Additionally volume and continuum extrapolations using three-flavor  $\chi$ PT cannot be trusted. Indeed the first lattice calculation of hyperon axial charges,  $g_{\Sigma\Sigma}$  and  $g_{\Xi\Xi}$  [31, 32], shows little evidence for the one-loop predictions from (partially quenched)  $\chi$ PT [33]. The lattice, however, can provide a diagnostic tool to investigate the condition of three-flavor  $\chi$ PT. A complete study of baryon axial charges is the natural starting point. These couplings enter in the loop graphs that determine the long-range chiral corrections to all baryon observables. Input of these measured parameters into  $\chi$ PT expressions allows one to numerically assess the behavior of the long-range contributions in the chiral expansion. This information can then be used to address the convergence of the chiral expansion. Perhaps the expansion is converging to the wrong answer, or perhaps the expansion is not converging at all. If it is the latter case, one can use the lattice to investigate the cause. Perhaps certain observables are corrupted by large values of local contributions that can be isolated and determined from lattice data, or perhaps nearby resonances are leading to large enhancements.

In this work, we provide a follow-up to [33] by determining the full set of hyperon matrix elements of flavor changing axial currents. We work to next-to-leading order in partially

quenched heavy baryon chiral perturbation theory to address both the chiral behavior and momentum-transfer dependence of the axial form factors. Due to meson pole contributions, the pseudoscalar form factor provides an observable well-suited for the investigation of chiral physics in three-flavor theories. Despite the accumulation of a large number (eight) of undetermined low-energy constants, we utilize the full set of axial charges to make non-trivial next-to-leading order predictions.

Our paper is organized as follows. First in Sect. II, aspects of  $\text{PQ}\chi\text{PT}$  relevant to our calculations are reviewed. In Sect. III, we map the  $\text{PQQCD}$  axial-vector current onto operators in  $\text{PQ}\chi\text{PT}$  up to next-to-leading order. The hyperon axial-current matrix elements are determined for  $|\Delta I| = 1$  transitions (Sect. III B), and  $|\Delta S| = 1$  transitions (Sect. III C). Various wavefunction renormalization factors are collected in the Appendix. Non-trivial next-to-leading order predictions for axial charges, and a discussion of  $SU(3)$  breaking corrections are presented in Sect. IV, which concludes our paper.

## II. PARTIALLY QUENCHED CHIRAL LAGRANGIAN

Before we detail the calculation of the axial current matrix elements, we briefly review partially quenched chiral perturbation theory. We recall the partially quenched chiral Lagrangian in the meson sector first and emphasize the relation between lattice measured meson masses and the parameters of the Lagrangian. The baryon Lagrangian is then described in detail.

### A. Mesons

The lattice action we consider here is comprised of valence and sea quarks, each of which comes in three flavors. In the continuum limit, this action can be described by the partially quenched QCD (PQQCD) Lagrange density, which is given by

$$\mathcal{L} = \overline{Q} i \not{D} Q - \overline{Q} m_Q Q, \quad (1)$$

where the quark fields appear in the vector  $Q$ , which has entries

$$Q = (u, d, s, j, l, r, \tilde{u}, \tilde{d}, \tilde{s})^T, \quad (2)$$

and transforms in the fundamental representation of the graded group  $SU(6|3)$ . The quark components of the field  $Q$  satisfy the following graded equal-time commutation relation

$$Q_i^\alpha(\mathbf{x}) Q_k^{\beta\dagger}(\mathbf{y}) - (-)^{\eta_i \eta_k} Q_k^{\beta\dagger}(\mathbf{y}) Q_i^\alpha(\mathbf{x}) = \delta^{\alpha\beta} \delta_{ik} \delta^3(\mathbf{x} - \mathbf{y}), \quad (3)$$

where  $(\alpha, \beta)$  and  $(i, k)$  are spin and flavor indices respectively. The  $\eta_k$ 's appearing above are given by  $\eta_k = +1$  for  $k = 1\text{--}6$  and  $\eta_k = 0$  for  $k = 7\text{--}9$ . The  $\eta_k$  maintain the graded structure of the Lie algebra. Further, the graded equal-time commutation relations for two  $Q$ 's or two  $Q^\dagger$ 's vanish. The partially quenched generalization of the mass matrix  $m_Q$  is given by

$$m_Q = \text{diag}(m_u, m_d, m_s, m_j, m_l, m_s, m_u, m_d, m_s). \quad (4)$$

In this work, we enforce the isospin limit in both the valence and sea sectors so that we have

$$m_Q = \text{diag}(\bar{m}, \bar{m}, m_s, m_j, m_j, m_s, \bar{m}, \bar{m}, m_s). \quad (5)$$

Notice that with Eq. (4) (and similarly Eq. (5)), there is an exact cancelation between valence and ghost quark contributions to the determinant in the path integral for the QCD partition function. This cancelation leaves only the contribution from the sea sector. When  $m_Q = 0$ , the Lagrangian Eq. (1) has a graded  $U(6|3)_L \otimes U(6|3)_R$  symmetry which will reduce to  $SU(6|3)_L \otimes SU(6|3)_R \otimes U(1)_V$  by the axial anomaly [5]. We assume that the chiral symmetry is spontaneously broken:  $SU(6|3)_L \otimes SU(6|3)_R \rightarrow SU(6|3)_V$ , hence an identification between PQQCD and QCD can be made. The low-energy effective theory of PQQCD is written in terms of the pseudo-Goldstone mesons emerging from spontaneous chiral symmetry breaking. At leading order in an expansion in momentum and quark mass,<sup>1</sup> the  $\text{PQ}\chi\text{PT}$  Lagrangian for the mesons is given by

$$\mathcal{L} = \frac{f^2}{8} \text{str} \left( \partial^\mu \Sigma^\dagger \partial_\mu \Sigma \right) + \lambda \text{str} \left( m_q \Sigma^\dagger + m_q^\dagger \Sigma \right) - m_0^2 \Phi_0^2, \quad (6)$$

where  $f = 132$  MeV, the  $\text{str}()$  denotes a graded flavor trace and the meson fields is incorporated in  $\Sigma$  through

$$\Sigma = \exp \left( \frac{2i\Phi}{f} \right) = \xi^2, \quad \Phi = \begin{pmatrix} M & \chi^\dagger \\ \chi & \tilde{M} \end{pmatrix}. \quad (7)$$

The matrices  $M, \tilde{M}$  in Eq. (7) contain bosonic mesons, while  $\chi$  and  $\chi^\dagger$  are matrices consisting of fermionic mesons. Here  $\Phi_0 = \text{str}(\Phi)\sqrt{6}$  is the flavor singlet field and is included as a device to obtain the flavor neutral propagators in  $\text{PQ}\chi\text{PT}$ . Expanding the Lagrangian in Eq. (6), one can determine the meson masses which enter into the calculations of baryon observables. In particular, the masses of mesons at leading order with quark content  $Q_i \bar{Q}'_j$  are

$$m_{Q_i Q'_j}^2 = \frac{4\lambda}{f^2} ((m_Q)_{ii} + (m_{Q'})_{jj}). \quad (8)$$

The flavor singlet field additionally acquires a mass  $m_0^2$ . Due to the strong  $U(1)_A$  anomaly, this mass can be taken on the order of the chiral symmetry breaking scale,  $m_0 \sim \Lambda_\chi \approx 4\pi f$ . The flavor singlet field can thus be integrated out. However, the propagator of the flavor neutral fields deviate from a simple pole form [5]. For  $a, b = u, d, s$ , the  $\eta_a \eta_b$  propagator at leading order is given by [5]

$$\mathcal{G}_{\eta_a \eta_b} = \frac{i\delta^{ab}}{q^2 - m_{aa}^2 + i\epsilon} - \frac{i}{3} \frac{(q^2 - m_{jj}^2 + i\epsilon)(q^2 - m_{rr}^2 + i\epsilon)}{(q^2 - m_{aa}^2 + i\epsilon)(q^2 - m_{bb}^2 + i\epsilon)(q^2 - m_X^2 + i\epsilon)}, \quad (9)$$

where the masses of valence-valence mesons  $m_{aa}^2, m_{bb}^2$  and the masses of the sea-sea mesons  $m_{jj}^2, m_{rr}^2$  are given by Eq. (8). In Eq. (9), the mass  $m_X$  is defined as  $m_X^2 = \frac{1}{3}(m_{jj}^2 + 2m_{rr}^2)$ . The flavor neutral propagator Eq. (9) can be conveniently written in the form

$$\mathcal{G}_{\eta_a \eta_b} = \delta^{ab} P_a + \mathcal{H}_{aa}(P_a, P_b, P_X), \quad (10)$$

---

<sup>1</sup> Here we adopt the standard power counting:  $\partial^2 \sim m_q \sim \varepsilon^2$ , where  $\varepsilon$  is a small parameter.

with

$$\begin{aligned}
P_a &= \frac{i}{q^2 - m_{aa}^2 + i\epsilon}, \quad P_b = \frac{i}{q^2 - m_{bb}^2 + i\epsilon}, \quad P_X = \frac{i}{q^2 - m_X^2 + i\epsilon}, \\
\mathcal{H}_{ab}(A, B, C) &= -\frac{1}{3} \left[ \frac{(m_{jj}^2 - m_{aa}^2)(m_{rr}^2 - m_{aa}^2)}{(m_{aa}^2 - m_{bb}^2)(m_{aa}^2 - m_X^2)} A - \frac{(m_{jj}^2 - m_{bb}^2)(m_{rr}^2 - m_{bb}^2)}{(m_{aa}^2 - m_{bb}^2)(m_{bb}^2 - m_X^2)} B \right. \\
&\quad \left. + \frac{(m_X^2 - m_{jj}^2)(m_X^2 - m_{rr}^2)}{(m_X^2 - m_{aa}^2)(m_X^2 - m_{bb}^2)} C \right]. \tag{11}
\end{aligned}$$

The above form is convenient for contributions from flavor neutral mixing. When there is no mixing, i.e.  $a = b$  and  $A = B$ , the hairpin propagator has a double pole and the limit of Eq. (11) must be taken, and produces

$$\begin{aligned}
\mathcal{H}_{aa}(A, A, C) &= -\frac{1}{3} \left[ \frac{\partial}{\partial m_{aa}^2} \frac{(m_{jj}^2 - m_{aa}^2)(m_{rr}^2 - m_{aa}^2)}{(m_{aa}^2 - m_X^2)} A \right. \\
&\quad \left. + \frac{(m_{jj}^2 - m_X^2)(m_{rr}^2 - m_X^2)}{(m_X^2 - m_{aa}^2)^2} C \right]. \tag{12}
\end{aligned}$$

In partially quenched simulations, one numerically determines the values of the valence pion  $m_{\pi,\text{val}}$  and valence kaon  $m_{K,\text{val}}$  masses, as well as the sea pion  $m_{\pi,\text{sea}}$  and sea kaon  $m_{K,\text{sea}}$  masses. When one uses PQ $\chi$ PT to calculate the meson mass dependence of observables, they are expressed in terms of meson masses via the tree-level relation in Eq. (8). To use the lattice determined meson masses in the valence and sea sectors, it is straightforward algebra to convert the loop meson masses appearing in PQ $\chi$ PT to those measured directly on the lattice. Explicitly we have

$$\begin{aligned}
m_{uu}^2 &= m_{\eta_u}^2 = m_{\pi,\text{val}}^2, \\
m_{us}^2 &= m_{K,\text{val}}^2, \\
m_{ss}^2 &= m_{\eta_s}^2 = 2m_{K,\text{val}}^2 - m_{\pi,\text{val}}^2, \\
m_{uj}^2 &= \frac{1}{2} (m_{\pi,\text{val}}^2 + m_{\pi,\text{sea}}^2), \\
m_{ur}^2 &= \frac{1}{2} (m_{\pi,\text{val}}^2 - m_{\pi,\text{sea}}^2) + m_{K,\text{sea}}^2, \\
m_{sj}^2 &= \frac{1}{2} (m_{\pi,\text{sea}}^2 - m_{\pi,\text{val}}^2) + m_{K,\text{val}}^2, \\
m_{sr}^2 &= -\frac{1}{2} (m_{\pi,\text{val}}^2 + m_{\pi,\text{sea}}^2) + m_{K,\text{val}}^2 + m_{K,\text{sea}}^2, \\
m_{jj}^2 &= m_{\pi,\text{sea}}^2, \\
m_{rr}^2 &= 2m_{K,\text{sea}}^2 - m_{\pi,\text{sea}}^2, \\
m_X^2 &= \frac{4}{3}m_{K,\text{sea}}^2 - \frac{1}{3}m_{\pi,\text{sea}}^2. \tag{13}
\end{aligned}$$

These relations must be modified if the source of partial quenching is due to mixed lattice actions, see [34, 35, 36].

## B. Baryon

In this section, we discuss the baryon sector of  $PQ\chi$ PT in the framework of [37, 38, 39]. Building blocks for the baryon Lagrangian are the super-multiplets  $\mathcal{B}_{ijk}$  and  $\mathcal{T}_{ijk}^\mu$ . The **240**-dimensional super-multiplet of spin- $\frac{1}{2}$  baryons  $\mathcal{B}_{ijk}$  satisfies the following relations under the interchange of the flavor indices [37]

$$\mathcal{B}_{ijk} = (-)^{1+\eta_j\eta_k} \mathcal{B}_{ikj}, \mathcal{B}_{ijk} + (-)^{1+\eta_i\eta_j} \mathcal{B}_{jik} + (-)^{1+\eta_i\eta_j+\eta_j\eta_k+\eta_k\eta_i} \mathcal{B}_{kji} = 0, \quad (14)$$

and the familiar octet baryons are embeded in  $\mathcal{B}_{ijk}$  through [38, 39]

$$\mathcal{B}_{ijk} = \frac{1}{\sqrt{6}}(\epsilon_{ijl}B_k^l + \epsilon_{ikl}B_j^l), \quad (15)$$

where  $B$  is the octet baryon matrix

$$B = \begin{pmatrix} \frac{1}{\sqrt{6}}\Lambda + \frac{1}{\sqrt{2}}\Sigma^0 & \Sigma^+ & p \\ \Sigma^- & \frac{1}{\sqrt{6}}\Lambda - \frac{1}{\sqrt{2}}\Sigma^0 & n \\ \Xi^- & \Xi^0 & -\frac{2}{\sqrt{6}}\Lambda \end{pmatrix}. \quad (16)$$

The spin- $\frac{3}{2}$  resonances are contained in the the **138**-dimensional super-multiplet  $\mathcal{T}_{ijk}$ , which satisfies

$$\mathcal{T}_{ijk} = (-)^{1+\eta_i\eta_j} \mathcal{T}_{jik} = (-)^{1+\eta_j\eta_k} \mathcal{T}_{ikj}, \quad (17)$$

under the interchange of flavor indices [37]. Furthermore, one embeds the decuplet baryons in  $\mathcal{T}_{ijk}$  by

$$\mathcal{T}_{ijk} = T_{ijk}, \quad (18)$$

where  $T$  is totally symmetric tensor containing the decuplet resonances

$$\begin{aligned} T_{111} &= \Delta^{++}, \quad T_{112} = \frac{1}{\sqrt{3}}\Delta^+, \quad T_{122} = \frac{1}{\sqrt{3}}\Delta^0, \quad T_{222} = \Delta^-, \\ T_{113} &= \frac{1}{\sqrt{3}}\Sigma^{*,+}, \quad T_{123} = \frac{1}{\sqrt{6}}\Sigma^{*,0}, \quad T_{223} = \frac{1}{\sqrt{3}}\Sigma^{*,-}, \\ T_{133} &= \frac{1}{\sqrt{3}}\Xi^{*,0}, \quad T_{233} = \frac{1}{\sqrt{3}}\Xi^{*,-}, \quad T_{333} = \Omega^-. \end{aligned} \quad (19)$$

The free Lagrangian for the **240**-dimensional super-multiplet  $\mathcal{B}_{ijk}$  and the **138**-dimensional super-multiplet  $\mathcal{T}_{ijk}$  fields in  $SU(6|3)$   $PQ\chi$ PT is given by [39]

$$\begin{aligned} \mathcal{L} = & i(\bar{\mathcal{B}}v \cdot \mathcal{D}\mathcal{B}) + 2\alpha_M(\bar{\mathcal{B}}\mathcal{B}\mathcal{M}_+) + 2\beta_M(\bar{\mathcal{B}}\mathcal{M}_+\mathcal{B}) + 2\sigma_M(\bar{\mathcal{B}}\mathcal{B})\text{str}(\mathcal{M}_+) \\ & - i(\bar{\mathcal{T}}^\mu v \cdot \mathcal{D}\mathcal{T}_\mu) + \Delta(\bar{\mathcal{T}}^\mu\mathcal{T}_\mu) + 2\gamma_M(\bar{\mathcal{T}}^\mu\mathcal{M}_+\mathcal{T}_\mu) - 2\bar{\sigma}_M(\bar{\mathcal{T}}^\mu\mathcal{T}_\mu)\text{str}(\mathcal{M}_+), \end{aligned} \quad (20)$$

where the mass operator  $\mathcal{M}_+$  is defined by:

$$\mathcal{M}_+ = \frac{1}{2}(\xi^\dagger m_Q \xi^\dagger + \xi m_Q \xi). \quad (21)$$

The parameter  $\Delta$  is the mass splitting between the octet and decuplet baryons in the chiral limit. Phenomenologically we know  $\Delta \sim m_\phi$ , where  $\phi$  is an  $SU(3)$  meson, hence the decuplet baryons must be included as dynamical fields in Eq. (20). The parenthesis notation for flavor contractions used in Eq. (20) is that of [39]. The partially quenched Lagrangian describing the interactions of the  $\mathcal{B}_{ijk}$  and  $\mathcal{T}_{ijk}^\mu$  with the pseudo-Goldstone mesons is given by [39]

$$\begin{aligned}\mathcal{L} = & 2\alpha \left( \overline{\mathcal{B}} S^\mu \mathcal{B} A_\mu \right) + 2\beta \left( \overline{\mathcal{B}} S^\mu A_\mu \mathcal{B} \right) + 2\mathcal{H} \left( \overline{\mathcal{T}}^\nu S^\mu A_\mu \mathcal{T}_\nu \right) \\ & + \sqrt{\frac{3}{2}} \mathcal{C} \left[ \left( \overline{\mathcal{T}}^\nu A_\nu \mathcal{B} \right) + \left( \overline{\mathcal{B}} A_\nu \mathcal{T}^\nu \right) \right].\end{aligned}\quad (22)$$

The axial-vector and vector meson fields  $A_\mu$  and  $V_\mu$  are defined by:  $A_\mu = \frac{i}{2} (\xi \partial_\mu \xi^\dagger - \xi^\dagger \partial_\mu \xi)$  and  $V_\mu = \frac{1}{2} (\xi \partial_\mu \xi^\dagger + \xi^\dagger \partial_\mu \xi)$ . The latter appears in Eq. (20) for the covariant derivatives of  $\mathcal{B}_{ijk}$  and  $\mathcal{T}_{ijk}$  that both have the form

$$(\mathcal{D}^\mu \mathcal{B})_{ijk} = \partial^\mu \mathcal{B}_{ijk} + (V^\mu)_i^l \mathcal{B}_{ljk} + (-)^{\eta_i(\eta_j + \eta_m)} (V^\mu)_j^m \mathcal{B}_{imk} + (-)^{(\eta_i + \eta_j)(\eta_k + \eta_n)} (V^\mu)_k^n \mathcal{B}_{ijn}. \quad (23)$$

The vector  $S_\mu$  is the covariant spin operator [18, 19]. The parameters that appear in the  $\text{PQ}\chi\text{PT}$  Lagrangian can be related to those in  $\chi\text{PT}$  by matching. To be more specific, one restricts to the  $q_{\text{sea}} q_{\text{sea}} q_{\text{sea}}$  sector and compares the  $\text{PQ}\chi\text{PT}$  Lagrangian obtained with that of  $\chi\text{PT}$ . With this matching procedure, one finds that  $\alpha = \frac{2}{3}D + 2F$ ,  $\beta = -\frac{5}{3}D + F$ , and the other parameters  $\mathcal{C}$  and  $\mathcal{H}$  appearing above have the same numerical values as in  $\chi\text{PT}$  [39].

### III. THE AXIAL-VECTOR CURRENT

#### A. The Axial-Vector Current in $\text{PQ}\chi\text{PT}$

The baryon matrix elements of the axial-vector current,  $j_{\mu,5}^a = \overline{q} \lambda^a \gamma_\mu \gamma_5 q$ , have been studied extensively both on the lattice [8, 9] and  $\chi\text{PT}$  [10, 11, 12, 15, 16, 18, 19, 33, 40, 41, 46, 47, 48, 49, 50]. In  $\text{PQQCD}$ , the axial current is defined by  $J_{\mu,5}^a = \overline{Q} \overline{\lambda}^a \gamma_\mu \gamma_5 Q$ . In general, one must worry that the choice of supermatrices  $\overline{\lambda}^a$  is not unique even after the requirement  $\text{str}(\overline{\lambda}^a) = 0$  has been enforced. To be relevant for any practical lattice calculation, the choice of  $\text{PQQCD}$  matrices should maintain the cancelation of valence and ghost quark loops with an operator insertion [33, 51]. This is because otherwise the  $\text{PQQCD}$  theory corresponds to a lattice theory where twice the number of disconnected contractions must be calculated. However since we are only interested in flavor-changing operators, the self contractions of these operators automatically vanish. Thus we can decouple the ghost and sea quarks sectors from the flavor changing axial current by choosing the upper  $3 \times 3$  block of  $\overline{\lambda}$  to be the Gell-Mann matrices. This choice merely corresponds to an axial transition operator that only acts in the valence sector and is precisely what is implemented on the lattice.<sup>2</sup>

<sup>2</sup> Isospin symmetry allows one to relate isospin transition matrix elements to differences of flavor conserving matrix elements. These difference have often been calculated on the lattice. For strangeness transitions,  $SU(3)$  is badly broken disallowing the analogous procedure.

Having fixed the  $\bar{\lambda}$  supermatrices, we map the PQQCD axial current operator into the heavy baryon PQ $\chi$ PT. At leading order, the PQ $\chi$ PT axial current is given by [10]

$$\begin{aligned} J_{\mu,5}^a &= 2\alpha \left( \bar{\mathcal{B}} S_\mu \mathcal{B} \bar{\lambda}_{\xi+}^a \right) + 2\beta \left( \bar{\mathcal{B}} S_\mu \bar{\lambda}_{\xi+}^a \mathcal{B} \right) + 2\mathcal{H} \left( \bar{\mathcal{T}}^\nu S_\mu \bar{\lambda}_{\xi+}^a \mathcal{T}_\nu \right) \\ &+ \sqrt{\frac{3}{2}} \mathcal{C} \left[ \left( \bar{\mathcal{T}}_\mu \bar{\lambda}_{\xi+}^a \mathcal{B} \right) + \left( \bar{\mathcal{B}} \bar{\lambda}_{\xi+}^a \mathcal{T}_\mu \right) \right]. \end{aligned} \quad (24)$$

with  $\alpha$ ,  $\beta$ ,  $\mathcal{H}$  and  $\mathcal{C}$  the same low energy constants (LEC's) appearing in Eq. (22) and  $\bar{\lambda}_{\xi+}^a = \frac{1}{2}(\xi \bar{\lambda}^a \xi^\dagger + \xi^\dagger \bar{\lambda}^a \xi)$ . Since we work to next-to-leading order (NLO) in the chiral expansion and NLO in the momentum expansion, we further require the contributions to the matrix elements from NLO axial current. At NLO, there are two contributions to the axial matrix elements: one is from the NLO axial current in the baryon sector and the other is obtained from the local counterterms involving one insertion of the quark mass matrix  $m_Q$ . The former is given by

$$\begin{aligned} J_{\mu,5}^a &= \frac{1}{\Lambda_\chi^2} \left\{ 2n_\alpha \left[ \partial_\mu \partial_\nu \left( \bar{\mathcal{B}} S^\nu \mathcal{B} \bar{\lambda}_{\xi+}^a \right) - \partial^2 \left( \bar{\mathcal{B}} S_\mu \mathcal{B} \bar{\lambda}_{\xi+}^a \right) \right] \right. \\ &\quad \left. + 2n_\beta \left[ \partial_\mu \partial_\nu \left( \bar{\mathcal{B}} S^\nu \bar{\lambda}_{\xi+}^a \mathcal{B} \right) - \partial^2 \left( \bar{\mathcal{B}} S_\mu \bar{\lambda}_{\xi+}^a \mathcal{B} \right) \right] \right\}. \end{aligned} \quad (25)$$

while the latter reads [10]:

$$\begin{aligned} J_{\mu,5}^{a,m_Q} &= 16 \frac{\lambda}{f^2} \left[ b_1 \bar{\mathcal{B}}^{kji} \{ \bar{\lambda}_{\xi+}^a, \mathcal{M}_+ \}_i^n S_\mu \mathcal{B}_{njk} + b_2 (-)^{(\eta_i + \eta_j)(\eta_k + \eta_n)} \bar{\mathcal{B}}^{kji} \{ \bar{\lambda}_{\xi+}^a, \mathcal{M}_+ \}_k^n S_\mu \mathcal{B}_{ijn} \right. \\ &+ b_3 (-)^{\eta_i(\eta_j + \eta_n)} \bar{\mathcal{B}}^{kji} (\bar{\lambda}_{\xi+}^a)_i^l (\mathcal{M}_+)_j^n S_\mu \mathcal{B}_{lnk} \\ &+ b_4 (-)^{\eta_i \eta_j + 1} \bar{\mathcal{B}}^{kji} \left( (\bar{\lambda}_{\xi+}^a)_i^l (\mathcal{M}_+)_j^n + (\mathcal{M}_+)_i^l (\bar{\lambda}_{\xi+}^a)_j^n \right) S_\mu \mathcal{B}_{nlk} \\ &+ b_5 (-)^{\eta_i(\eta_l + \eta_j)} \bar{\mathcal{B}}^{kji} (\bar{\lambda}_{\xi+}^a)_j^l (\mathcal{M}_+)_i^n S_\mu \mathcal{B}_{nlk} + b_6 \bar{\mathcal{B}}^{kji} (\bar{\lambda}_{\xi+}^a)_i^l S_\mu \mathcal{B}_{ljk} \text{ str}(\mathcal{M}_+) \\ &+ b_7 (-)^{(\eta_i + \eta_j)(\eta_k + \eta_n)} \bar{\mathcal{B}}^{kji} (\bar{\lambda}_{\xi+}^a)_k^n S_\mu \mathcal{B}_{ijn} \text{ str}(\mathcal{M}_+) \\ &\quad \left. + b_8 \bar{\mathcal{B}}^{kji} S_\mu \mathcal{B}_{ijk} \text{ str}(\bar{\lambda}_{\xi+}^a \mathcal{M}_+) \right], \end{aligned} \quad (26)$$

where the coefficients  $b_1, b_2, \dots, b_8$  must be determined from lattice simulations. The relation between the partially quenched parameters  $n_\alpha, n_\beta$  and the physical parameters  $n_D, n_F$  in usual  $SU(3)$   $\chi$ PT can be obtained by matching:  $n_\alpha = \frac{2}{3}n_D + 2n_F$ ,  $n_\beta = -\frac{5}{3}n_D + n_F$ . Notice that the operator  $b_8 \bar{\mathcal{B}}^{kji} S_\mu \mathcal{B}_{ijk} \text{ str}(\bar{\lambda}_{\xi+}^a \mathcal{M}_+)$  does not contribute to the flavor changing transitions at tree-level. This leaves seven independent partially quenched NLO operators, one more than that in ordinary  $SU(3)$ . However, because these counterterms only contribute to tree-level, no unphysical combinations will be introduced.

## B. Isospin Changing Transitions

In the partially quenched theory, the supermatrix for the  $\Delta I = 1$  isospin changing transitions is

$$\bar{\lambda}_{ij}^{1+2i} = \begin{cases} 1 & i = 1, j = 2 \\ 0 & \text{otherwise} \end{cases}. \quad (27)$$

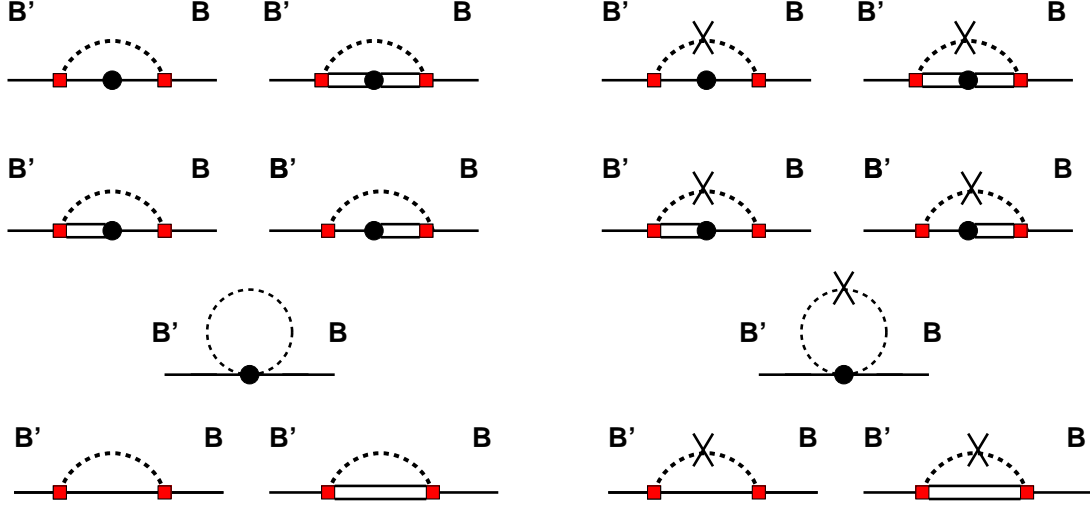


FIG. 1: One-loop diagrams which contribute to the leading non-analytic terms of the octet baryon axial form factors. Mesons are represented by a dashed line while the single and double lines are the symbols for an octet and a decuplet respectively. The solid circle is an insertion of the axial current operator and the solid squares are the couplings given in Eq. (22). The wave function renormalization diagrams are depicted in the bottom row. The diagrams with a cross on the loop meson are the hairpin contributions which arise from the flavor neutral meson propagators.

Within the baryon octet there are six isospin  $\Delta I = 1$  changing transitions, namely

$$n \rightarrow p, \Sigma^0 \rightarrow \Sigma^+, \Sigma^- \rightarrow \Sigma^0, \Lambda \rightarrow \Sigma^+, \Sigma^- \rightarrow \Lambda, \Xi^- \rightarrow \Xi^0. \quad (28)$$

The neutron to proton axial transition defines the nucleon axial form factor  $G_{A,NN}(q^2)$  and induced pseudoscalar form factor  $G_{P,NN}(q^2)$

$$\langle p(P') | J_{\mu,5}^{1+2i} | n(P) \rangle = \overline{U}_N(P') \left[ 2S_\mu G_{A,NN}(q^2) + \frac{q_\mu q \cdot S}{(2m_N)^2} G_{P,NN}(q^2) \right] U_N(P), \quad (29)$$

where  $q_\mu = (P' - P)_\mu$  is the four momentum transfer. The  $\Sigma\Sigma$  transition matrix elements define the  $\Sigma\Sigma$  axial form factor  $G_{A,\Sigma\Sigma}(q^2)$  and induced pseudoscalar form factor  $G_{P,\Sigma\Sigma}(q^2)$

$$\langle \Sigma^0(P') | J_{\mu,5}^{1+2i} | \Sigma^-(P) \rangle = \frac{1}{\sqrt{2}} \overline{U}_\Sigma(P') \left[ 2S_\mu G_{A,\Sigma\Sigma}(q^2) + \frac{q_\mu q \cdot S}{(2m_\Sigma)^2} G_{P,\Sigma\Sigma}(q^2) \right] U_\Sigma(P). \quad (30)$$

While there are two  $\Sigma\Sigma$  isospin transitions, their matrix elements are related by isospin algebra

$$\langle \Sigma^+(P') | J_{\mu,5}^{1+2i} | \Sigma^0(P) \rangle = -\langle \Sigma^0(P') | J_{\mu,5}^{1+2i} | \Sigma^-(P) \rangle. \quad (31)$$

The  $\Lambda\Sigma$  transition matrix elements define the  $\Lambda\Sigma$  axial form factor  $G_{A,\Lambda\Sigma}$  and induced pseudoscalar form factor  $G_{P,\Lambda\Sigma}(q^2)$

$$\langle \Lambda(P') | J_{\mu,5}^{1+2i} | \Sigma^-(P) \rangle = \frac{1}{\sqrt{6}} \overline{U}_\Lambda(P') \left[ 2S_\mu G_{A,\Lambda\Sigma}(q^2) + \frac{q_\mu q \cdot S}{(m_\Lambda + m_\Sigma)^2} G_{P,\Lambda\Sigma}(q^2) \right] U_\Sigma(P). \quad (32)$$

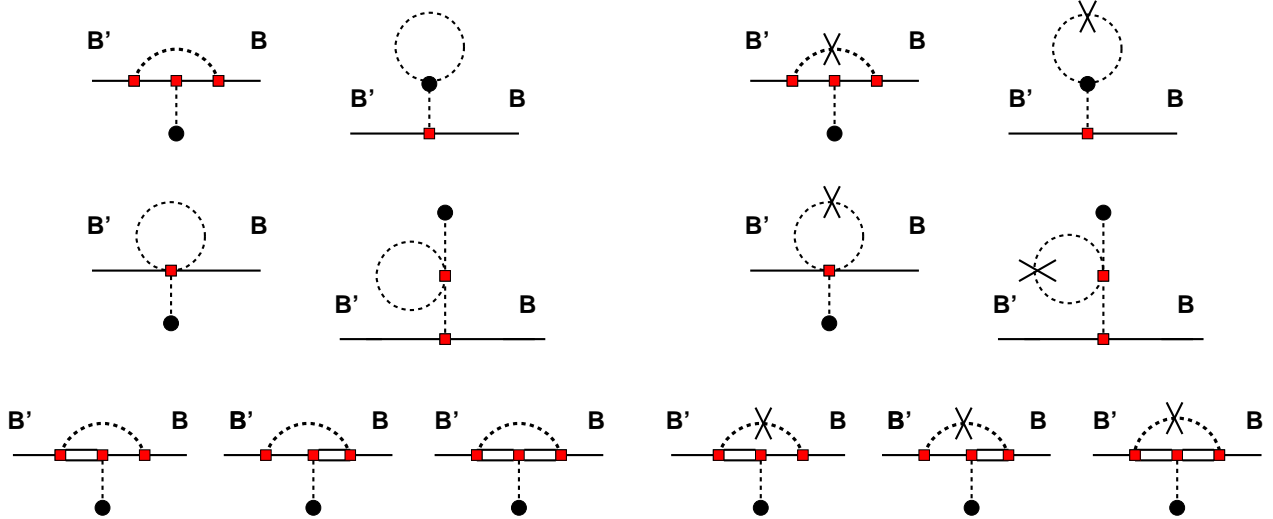


FIG. 2: One-loop diagrams which contribute to the leading non-analytic terms of the octet baryon induced pseudoscalar form factors. Diagram elements are the same as FIG. 1

Although there are two  $\Lambda\Sigma$  transition matrix elements, they are related by isospin

$$\langle \Sigma^+(P') | J_{\mu,5}^{1+2i} | \Lambda(P) \rangle = \langle \Lambda(P') | J_{\mu,5}^{1+2i} | \Sigma^-(P) \rangle. \quad (33)$$

Finally, the  $\Xi\Xi$  axial form factor  $G_{A,\Xi\Xi}$  and induced pseudoscalar form factor  $G_{P,\Lambda\Sigma}(q^2)$  appear in the  $\Xi\Xi$  transition matrix element

$$\langle \Xi^0(P') | J_{\mu,5}^{1+2i} | \Xi^-(P) \rangle = \overline{U}_\Xi(P') \left[ 2S_\mu G_{A,\Xi\Xi}(q^2) + \frac{q_\mu q \cdot S}{(2m_\Xi)^2} G_{P,\Xi\Xi}(q^2) \right] U_\Xi(P). \quad (34)$$

Here we use heavy baryon spinors and notation. One can easily show up to recoil corrections,  $2\overline{U}(P')S_\mu U(P) = \overline{U}(P')\gamma_\mu\gamma_5 U(P)$ , where on the right-hand side appears ordinary Dirac matrices and spinors. Thus the axial charges,  $G_{A,B'B}(0)$ , are the standard ones. In our power counting, while the tree-level contributions from LO axial current is of order  $\varepsilon^0$ , the tree-level contributions obtained from NLO current count  $\varepsilon^2$ . In addition, at order  $\varepsilon^2$  there are leading non-analytic contributions to the matrix elements from the one-loop diagrams shown in Fig. 1 and Fig. 2. The one-loop diagrams in Fig. 1 contribute to the axial form factors while the induced pseudoscalar form factors receive contributions from the one-loop diagrams in Fig. 2. Evaluation of the diagrams in Fig. 1 together with the tree-level contributions yields the following expression for the axial form factor of  $\Delta I = 1$

isospin transitions

$$\begin{aligned}
G_{A,B'B}(q^2) = & g_{B'B} \sqrt{Z_{B'} Z_B} + \frac{1}{16\pi^2 f^2} \left[ g_{B'B} \sum_{\phi} C_{\phi} \mathcal{L}(m_{\phi}, \mu) \right. \\
& + \mathcal{H} \mathcal{C}^2 \left( \sum_{\phi} E_{\phi} \mathcal{J}(m_{\phi}, \Delta, \mu) + \sum_{\phi\phi'} \bar{E}_{\phi\phi'} \mathcal{T}(\eta_{\phi} \eta_{\phi'}, \Delta, \mu) \right) \\
& + \mathcal{C}^2 \left( \sum_{\phi} A_{\phi} \mathcal{K}(m_{\phi}, \Delta, \mu) + \sum_{\phi\phi'} \bar{A}_{\phi\phi'} \mathcal{S}(\eta_{\phi} \eta_{\phi'}, \Delta, \mu) \right) \\
& + \sum_{\phi} Y_{\phi} \mathcal{L}(m_{\phi}, \mu) + \sum_{\phi\phi'} \bar{Y}_{\phi\phi'} \mathcal{R}(\eta_{\phi} \eta_{\phi'}, \Delta, \mu) \left. \right] \\
& + n_{B'B} \frac{q^2}{\Lambda_{\chi}^2} + \sum_{\phi} u_{\phi} m_{\phi}^2. \tag{35}
\end{aligned}$$

In Eq. (35),  $B$  ( $B'$ ) stands for the initial (final) octet baryon,  $Z_B$  and  $Z_{B'}$  are the wave function renormalization factors and are given in the Appendix. The constants  $g_{B'B}$ 's are the leading order octet baryon axial charges

$$g_{NN} = (D + F), \quad g_{\Lambda\Sigma} = 2D, \quad g_{\Xi\Xi} = (D - F), \quad g_{\Sigma\Sigma} = 2F, \tag{36}$$

and the coefficients  $n_{B'B}$  are given by

$$n_{NN} = n_D + n_F, \quad n_{\Lambda\Sigma} = 2n_D, \quad n_{\Xi\Xi} = n_D - n_F, \quad n_{\Sigma\Sigma} = 2n_F. \tag{37}$$

The coefficients  $C_{\phi}$ ,  $E_{\phi}$ ,  $\bar{E}_{\phi\phi'}$ ,  $A_{\phi}$ ,  $\bar{A}_{\phi\phi'}$ ,  $Y_{\phi}$ ,  $\bar{Y}_{\phi\phi'}$  are given in tables I, II, III, IV and V while the non-analytic functions appearing in Eq. (35), namely,  $\mathcal{L}$ 's,  $\mathcal{J}$ 's,  $\mathcal{K}$ 's,  $\mathcal{R}$ 's,  $\mathcal{T}$ 's and  $\mathcal{S}$ 's are given by

$$\begin{aligned}
\mathcal{L}(m, \mu) = & m^2 \log \left( \frac{m^2}{\mu^2} \right), \\
\tag{38}
\end{aligned}$$

$$\begin{aligned}
\mathcal{K}(m, \Delta, \mu) = & \left( m^2 - \frac{2}{3} \Delta^2 \right) \log \left( \frac{m^2}{\mu^2} \right) \\
& + \frac{2}{3} \Delta \sqrt{\Delta^2 - m^2} \log \left( \frac{\Delta - \sqrt{\Delta^2 - m^2 + i\epsilon}}{\Delta + \sqrt{\Delta^2 - m^2 + i\epsilon}} \right) \\
& + \frac{2}{3} \frac{m^2}{\Delta} \left( \pi m - \sqrt{\Delta^2 - m^2} \log \left( \frac{\Delta - \sqrt{\Delta^2 - m^2 + i\epsilon}}{\Delta + \sqrt{\Delta^2 - m^2 + i\epsilon}} \right) \right), \tag{39}
\end{aligned}$$

$$\begin{aligned}
\mathcal{J}(m, \Delta, \mu) = & \left( m^2 - 2\Delta^2 \right) \log \left( \frac{m^2}{\mu^2} \right) \\
& + 2\Delta \sqrt{\Delta^2 - m^2} \log \left( \frac{\Delta - \sqrt{\Delta^2 - m^2 + i\epsilon}}{\Delta + \sqrt{\Delta^2 - m^2 + i\epsilon}} \right), \tag{40}
\end{aligned}$$

$$\begin{aligned}
\mathcal{R}(\eta_\phi \eta_{\phi'}, \Delta, \mu) &= \mathcal{H}(\mathcal{L}(m_{\eta_\phi}, \mu), \mathcal{L}(m_{\eta_{\phi'}}, \mu), \mathcal{L}(m_X, \mu)), \\
\mathcal{T}(\eta_\phi \eta_{\phi'}, \Delta, \mu) &= \mathcal{H}(\mathcal{J}(m_{\eta_\phi}, \Delta, \mu), \mathcal{J}(m_{\eta_{\phi'}}, \Delta, \mu), \mathcal{J}(m_X, \Delta, \mu)), \\
\mathcal{S}(\eta_\phi \eta_{\phi'}, \Delta, \mu) &= \mathcal{H}(\mathcal{K}(m_{\eta_\phi}, \Delta, \mu), \mathcal{K}(m_{\eta_{\phi'}}, \Delta, \mu), \mathcal{K}(m_X, \Delta, \mu)). \tag{41}
\end{aligned}$$

At NLO, the momentum behavior of the axial form factors is purely polynomial. This in turn implies that the axial radii  $\langle r_{B'B}^2 \rangle$  which are defined by  $\langle r_{B'B}^2 \rangle \equiv \lim_{q \rightarrow 0} 6 \frac{d}{dq^2} G_{A,B'B}(q^2)$ , are insensitive to NLO chiral corrections. Since no  $q^2$  dependence appears in the non-analytic functions from one-loop diagrams, the axial form factors are insensitive to the long-range effects introduced by boundary conditions. Therefore, flavor twisted boundary conditions can be used to produce momentum transfer between initial and final baryon states without sizable finite volume corrections to the extraction of the axial radii [53].

The one-loop diagrams which contribute at NLO to the pseudoscalar form factor are depicted in Fig.2. Additionally there are further diagrams generated by the insertion of local interactions from the fourth-order meson Lagrangian. Despite the large number of diagrams, there are a number of simplifications. In particular the second and fourth diagrams of the second line in Fig. 2 (along with local insertions on the meson line) lead to the one-loop renormalized pion propagator. Additionally the second and fourth diagrams of the first row in Fig 2 (along with NLO pion axial coupling) contribute to the one-loop value of the pion decay constant. The remaining ten diagrams are generated from vertices in the NLO baryon Lagrangian. These diagrams renormalize the tree-level axial coupling of the pion to the baryons. Carefully accounting for all of these factors, we find

$$G_{P,B'B}(q^2) = (m_B + m_{B'})^2 \left( \frac{f_\pi/f}{q^2 - m_\pi^2} G_{A,B'B}(0) \sqrt{Z_\pi} - \frac{1}{3} \langle r_{B'B}^2 \rangle \right), \tag{42}$$

where in this NLO expression, the axial charge  $G_{A,B'B}(0)$ , pion mass  $m_\pi$  and pion decay constant  $f_\pi$  are taken to be their physical values and  $Z_\pi$  is the pion wavefunction renormalization which is shown in the Appendix. In fitting lattice data to Eq. (42), one would thus use the lattice measured values for  $G_{A,B'B}(0)$ ,  $m_\pi$  and  $f_\pi$ . The final term in the pseudoscalar form factor is  $\langle r_{B'B}^2 \rangle$ , which is the axial radius. Its appearance here was discovered long ago under the guise of PCAC by Adler and Dothan [52]

The simple structure of the psuedoscalar form factor at NLO in both  $\chi$ PT and  $\text{PQ}\chi$ PT allows one perform an approximate check of the Goldberger-Treiman relation. The residue of the pseudoscalar form factor at the pion pole is proportional to the pion-baryon-baryon coupling  $G_{\pi B'B}$ . One can thus perturbatively investigate the Goldberger-Treiman relation using a lattice determination of the pseudoscalar form factor. This indirect method is considerably simpler than a lattice measurement of baryon-to-baryon-plus-pion correlation functions which contain final state interactions.

$$\begin{array}{c} C_\phi \\ \hline u\bar{u} & u\bar{u} \\ -2 & -1 \end{array}$$

TABLE I: The coefficients  $C_\phi$  in  $\text{PQ}\chi$ PT for the isospin changing axial form factors. The  $C_\phi$  are categorized by the loop mesons  $\phi$  with mass  $m_\phi$  and are the same for all isospin transitions.

$E_\phi$								$\bar{E}_{\phi\phi'}$		
	$\eta_u$	$\eta_s$	$us$	$uj$	$ur$	$sj$	$sr$	$\eta_u\eta_u$	$\eta_u\eta_s$	$\eta_s\eta_s$
$NN$	$-\frac{20}{27}$	0	0	$-\frac{40}{81}$	$-\frac{20}{81}$	0	0	0	0	0
$\Lambda\Sigma$	$-\frac{10}{27}$	0	$-\frac{10}{54}$	$-\frac{10}{27}$	$-\frac{10}{54}$	0	0	0	0	0
$\Xi\Xi$	0	$\frac{5}{81}$	$\frac{10}{81}$	0	0	$\frac{10}{81}$	$\frac{5}{81}$	$\frac{10}{81}$	$-\frac{20}{81}$	$\frac{10}{81}$
$\Sigma\Sigma$	$-\frac{10}{81}$	0	$-\frac{65}{81}$	$-\frac{10}{81}$	$-\frac{5}{81}$	$-\frac{40}{81}$	$-\frac{20}{81}$	$-\frac{20}{81}$	$\frac{40}{81}$	$-\frac{20}{81}$

TABLE II: The coefficients  $E_\phi$  and  $\bar{E}_{\phi\phi'}$  in  $\text{PQ}\chi\text{PT}$  for the isospin changing axial form factors. The  $E_\phi$  are categorized by the loop mesons  $\phi$  with mass  $m_\phi$  and  $\bar{E}_{\phi\phi'}$  are listed by pairs  $\phi\phi'$  of  $\eta_q$  mesons.

$A_\phi$				$\bar{A}_{\phi\phi'}$		
	$\eta_u$	$\eta_s$	$us$	$uj$	$\eta_u\eta_u$	$\eta_u\eta_s$
$NN$	$\frac{8}{9}D + \frac{8}{3}F$	0	0	$\frac{8}{3}D + \frac{8}{9}F$	0	0
$\Lambda\Sigma$	$-\frac{4}{9}D + \frac{4}{3}F$	0	$\frac{16}{9}D + \frac{8}{3}F$	$\frac{16}{9}D$	$\frac{16}{9}D - \frac{8}{3}F$	$-\frac{20}{9}D + \frac{4}{3}F$
$\Xi\Xi$	0	$\frac{8}{9}F$	$\frac{4}{9}D + \frac{4}{9}F$	0	$\frac{8}{9}D - \frac{8}{9}F$	$-\frac{8}{9}D - \frac{8}{9}F$
$\Sigma\Sigma$	$\frac{8}{9}F$	0	$\frac{4}{9}D + \frac{4}{9}F$	$\frac{8}{9}D + \frac{8}{9}F$	$\frac{16}{9}F$	$-\frac{8}{9}D - \frac{8}{9}F$

	$ur$	$sj$	$sr$	$\eta_s\eta_s$
$NN$	$\frac{4}{3}D + \frac{4}{9}F$	0	0	0
$\Lambda\Sigma$	$\frac{8}{9}D$	$\frac{8}{9}D + \frac{8}{3}F$	$\frac{4}{9}D + \frac{4}{3}F$	$\frac{4}{9}D + \frac{4}{3}F$
$\Xi\Xi$	0	$\frac{16}{9}F$	$\frac{8}{9}F$	$\frac{16}{9}F$
$\Sigma\Sigma$	$\frac{4}{9}D + \frac{4}{9}F$	$\frac{16}{9}D - \frac{16}{9}F$	$\frac{8}{9}D - \frac{8}{9}F$	$\frac{8}{9}D - \frac{8}{9}F$

TABLE III: The coefficients  $A_\phi$  and  $\bar{A}_{\phi\phi'}$  in  $\text{PQ}\chi\text{PT}$  for the isospin changing axial form factors. The  $A_\phi$  and  $\bar{A}_{\phi\phi'}$  coefficients are categorized as in Table II.

### C. Strangeness Changing Transitions

The  $\Delta S = -1$  strangeness changing transitions corresponds to the flavor matrix  $\bar{\lambda}^{4+5i}$  which is given by

$$\bar{\lambda}_{ij}^{4+5i} = \begin{cases} 1 & i = 1, j = 3 \\ 0 & \text{otherwise} \end{cases}, \quad (43)$$

in the partially quenched theory. With Eq. (43) there exists six strangeness changing transitions among the hyperons

$$\Sigma^0 \rightarrow p, \Sigma^- \rightarrow n, \Lambda \rightarrow p, \Xi^0 \rightarrow \Sigma^+, \Xi^- \rightarrow \Sigma^0, \Xi^- \rightarrow \Lambda. \quad (44)$$

The  $N\Lambda$  transition matrix elements define the  $N\Lambda$  axial form factor  $G_{A,N\Lambda}(q^2)$  and induced pseudoscalar form factor  $G_{P,N\Lambda}(q^2)$

$$\langle p(P') | J_{\mu,5}^{4+5i} | \Lambda(P) \rangle = -\frac{1}{\sqrt{6}} \bar{U}_N(P') \left[ 2S_\mu G_{A,N\Lambda}(q^2) + \frac{q_\mu q \cdot S}{(m_N + m_\Lambda)^2} G_{P,N\Lambda}(q^2) \right] U_\Lambda(P), \quad (45)$$

$Y_\phi$			$\bar{Y}_{\phi\phi'}$
	$\eta_u$	$\eta_s$	$\eta_u\eta_u$
$NN$	$-\frac{4}{3}D^3 + \frac{16}{3}D^2F - 4DF^2$	0	$-D^3 + 5D^2F - 3DF^2 - 9F^3$
$\Lambda\Sigma$	$-\frac{16}{9}D^3 + \frac{16}{3}D^2F$	0	$\frac{16}{3}D^2F - 8DF^2$
$\Xi\Xi$	0	$-\frac{2}{9}D^3 - \frac{2}{3}D^2F - 2DF^2 + 2F^3$	$-D^3 + 3D^2F - 3DF^2 + F^3$
$\Sigma\Sigma$	$-\frac{8}{9}D^3 + \frac{4}{3}D^2F - 4F^3$	0	$-8F^3$
	$us$	$uj$	$\eta_u\eta_s$
$NN$	0	$\frac{4}{3}D^3 - \frac{4}{3}D^2F + 4DF^2 - 4F^3$	0
$\Lambda\Sigma$	$\frac{4}{9}D^3 - \frac{4}{3}D^2F$	$\frac{4}{9}D^3 - \frac{8}{3}D^2F + 4DF^2$	$-\frac{8}{3}D^3 + \frac{16}{3}D^2F - 8DF^2$
$\Xi\Xi$	$\frac{2}{9}D^3 - \frac{2}{3}D^2F + 6DF^2 - 2F^3$	0	$4D^2F - 8DF^2 + 4F^3$
$\Sigma\Sigma$	$-\frac{4}{9}D^3 + \frac{16}{3}D^2F - 8DF^2 + 4F^3$	$\frac{8}{9}D^3 + \frac{4}{3}D^2F - 4F^3$	$8DF^2 - 8F^3$
	$ur$	$sj$	$\eta_s\eta_s$
$NN$	$\frac{2}{3}D^3 - \frac{2}{3}D^2F + 2DF^2 - 2F^3$	0	0
$\Lambda\Sigma$	$\frac{2}{9}D^3 - \frac{4}{3}D^2F + 2DF^2$	$\frac{4}{3}D^3 + \frac{8}{3}D^2F - 4DF^2$	$\frac{2}{3}D^3 + \frac{4}{3}D^2F - 2DF^2$
$\Xi\Xi$	0	$\frac{4}{9}D^3 + \frac{4}{3}D^2F - 4DF^2 + 4F^3$	$-4DF^2 + 4F^3$
$\Sigma\Sigma$	$\frac{4}{9}D^3 + \frac{2}{3}D^2F - 2F^3$	$-4D^2F + 8DF^2 - 4F^3$	$-2D^2F + 4DF^2 - 2F^3$
	$sr$		
$NN$	0		
$\Lambda\Sigma$	$\frac{2}{3}D^3 + \frac{4}{3}D^2F - 2DF^2$		
$\Xi\Xi$	$\frac{2}{9}D^3 + \frac{2}{3}D^2F - 2DF^2 + 2F^3$		
$\Sigma\Sigma$	$-2D^2F + 4DF^2 - 2F^3$		

TABLE IV: The coefficients  $Y_\phi$  and  $\bar{Y}_{\phi\phi'}$  in PQ $\chi$ PT for the isospin changing axial form factors. The  $Y_\phi$  and  $\bar{Y}_{\phi\phi'}$  coefficients are categorized as in Table II.

$u_\phi$				
	$uu$	$ss$	$jj$	$rr$
$NN$	$-\frac{1}{3}b_1 + \frac{2}{3}b_2 - \frac{1}{6}b_3 + \frac{1}{6}b_4 + \frac{1}{3}b_5$	0	$\frac{2}{3}b_7 - \frac{1}{3}b_6$	$\frac{1}{3}b_7 - \frac{1}{6}b_6$
$\Lambda\Sigma$	$-b_1 + \frac{1}{2}b_2 - \frac{1}{4}b_3 + \frac{1}{4}b_5$	$-\frac{1}{4}b_3 + \frac{1}{2}b_4$	$\frac{1}{2}b_7 - b_6$	$\frac{1}{4}b_7 - \frac{1}{2}b_6$
$\Xi\Xi$	$-\frac{2}{3}b_1 - \frac{1}{6}b_2$	$-\frac{1}{3}b_3 + \frac{1}{3}b_4 - \frac{1}{12}b_5$	$-\frac{1}{6}b_7 - \frac{2}{3}b_6$	$-\frac{1}{12}b_7 - \frac{1}{3}b_6$
$\Sigma\Sigma$	$\frac{1}{3}b_1 + \frac{5}{6}b_2 + \frac{1}{12}b_3 + \frac{1}{6}b_4 + \frac{1}{12}b_5$	$\frac{1}{12}b_3 - \frac{1}{3}b_4 + \frac{1}{3}b_5$	$\frac{5}{6}b_7 + \frac{1}{3}b_6$	$\frac{5}{12}b_7 + \frac{1}{6}b_6$

TABLE V: The coefficients  $u_\phi$  in PQ $\chi$ PT for the isospin changing axial form factors. The  $u_\phi$  coefficients are categorized by the mesons with mass  $m_\phi$ .

where, as above  $q_\mu = (P' - P)_\mu$  is the four momentum transfer. The  $\Lambda\Xi$  transition matrix elements define the  $\Lambda\Xi$  axial form factor  $G_{A,\Lambda\Xi}$  and induced pseudoscalar form factor  $G_{P,\Lambda\Xi}$

$$\langle \Lambda(P') | J_{\mu,5}^{4+5i} | \Xi^-(P) \rangle = \frac{1}{\sqrt{6}} \overline{U}_\Lambda(P') \left[ 2S_\mu G_{A,\Lambda\Xi}(q^2) + \frac{q_\mu q \cdot S}{(m_\Lambda + m_\Xi)^2} G_{P,\Lambda\Xi}(q^2) \right] U_\Xi(P). \quad (46)$$

The  $N\Sigma$  axial transitions defines the  $N\Sigma$  axial form factor  $G_{A,N\Sigma}(q^2)$  and the induced pseudoscalar form factor  $G_{P,N\Sigma}(q^2)$

$$\langle n(P') | J_{\mu,5}^+ | \Sigma^-(P) \rangle = \overline{U}_N(P') \left[ 2S_\mu G_{A,N\Sigma}(q^2) + \frac{q_\mu q \cdot S}{(m_N + m_\Sigma)^2} G_{P,N\Sigma}(q^2) \right] U_\Sigma(P). \quad (47)$$

Finally, the  $\Sigma\Xi$  axial form factor  $G_{A,\Sigma\Xi}(q^2)$  and the induced pseudoscalar form factor  $G_{P,\Sigma\Xi}(q^2)$  is defined through the  $\Sigma\Xi$  transition matrix element

$$\langle \Sigma^0(P') | J_{\mu,5}^{4+5} | \Xi^-(P) \rangle = \frac{1}{\sqrt{2}} \overline{U}_\Sigma(P') \left[ 2S_\mu G_{A,\Sigma\Xi}(q^2) + \frac{q_\mu q \cdot S}{(m_\Sigma + m_\Xi)^2} G_{P,\Sigma\Xi}(q^2) \right] U_\Xi(P). \quad (48)$$

Notice while there are two  $N\Sigma$  and two  $\Sigma\Xi$  transitions, both of their matrix elements are related by isospin factors, namely:

$$\begin{aligned} \langle p(P') | J_{\mu,5}^{4+5i} | \Sigma^0(P) \rangle &= \frac{1}{\sqrt{2}} \langle n(P') | J_{\mu,5}^{4+5i} | \Sigma^-(P) \rangle, \\ \langle \Sigma^0(P') | J_{\mu,5}^{4+5i} | \Xi^-(P) \rangle &= \frac{1}{\sqrt{2}} \langle \Sigma^+(P') | J_{\mu,5}^{4+5i} | \Xi^0(P) \rangle. \end{aligned} \quad (49)$$

Following the same considerations in section III B and assembling the LO and NLO contributions, the axial form factors of strangeness changing transitions are given by

$$\begin{aligned} G_{A,B'B}(q^2) &= g_{B'B} \sqrt{Z_{B'} Z_B} + \frac{1}{16\pi^2 f^2} \left[ g_{B'B} \left( \sum_\phi C_\phi \mathcal{L}(m_\phi, \mu) \right. \right. \\ &\quad \left. \left. + \sum_{\phi\phi'} \bar{C}_{\phi\phi'} \mathcal{R}(\eta_\phi \eta_{\phi'}, \Delta, \mu) \right) + \mathcal{H} \mathcal{C}^2 \left( \sum_\phi E_\phi \mathcal{J}(m_\phi, \Delta, \mu) \right. \right. \\ &\quad \left. \left. + \sum_{\phi\phi'} \bar{E}_{\phi\phi'} \mathcal{T}(\eta_\phi \eta_{\phi'}, \Delta, \mu) \right) \right. \\ &\quad \left. + \mathcal{C}^2 \left( \sum_\phi A_\phi \mathcal{K}(m_\phi, \Delta, \mu) + \sum_{\phi\phi'} \bar{A}_{\phi\phi'} \mathcal{S}(\eta_\phi \eta_{\phi'}, \Delta, \mu) \right) \right. \\ &\quad \left. + \sum_\phi Y_\phi \mathcal{L}(m_\phi, \mu) + \sum_{\phi\phi'} \bar{Y}_{\phi,\phi'} \mathcal{R}(\eta_\phi \eta_{\phi'}, \Delta, \mu) \right] \\ &\quad + n_{B'B} \frac{q^2}{\Lambda_\chi^2} + \sum_\phi u_\phi m_\phi^2. \end{aligned} \quad (50)$$

In Eq. (50), we use  $B$  and  $B'$  to denote the initial and final states of octet baryon,  $Z_B$  and  $Z_{B'}$  are again the wave function renormalization for which the explicit expressions are

given in the Appendix. The  $g_{B'B}$ 's appearing above are the leading order octet baryon axial charges

$$\begin{aligned} g_{N\Lambda} &= (3F + D), \quad g_{\Lambda\Xi} = (3F - D), \\ g_{N\Sigma} &= (D - F), \quad g_{\Sigma\Xi} = (F + D), \end{aligned} \quad (51)$$

and the coefficients  $n_{B'B}$  are given by a formula of exactly the same form

$$\begin{aligned} n_{N\Lambda} &= 3n_F + n_D, \quad n_{\Lambda\Xi} = 3n_F - n_D, \\ n_{N\Sigma} &= n_D - n_F, \quad n_{\Sigma\Xi} = n_D + n_F. \end{aligned} \quad (52)$$

The coefficients  $C_\phi$ ,  $\bar{C}_{\phi\phi'}$ ,  $E_\phi$ ,  $\bar{E}_{\phi\phi'}$ ,  $A_\phi$ ,  $\bar{A}_{\phi\phi'}$ ,  $Y_\phi$ ,  $\bar{Y}_{\phi\phi'}$  are given in tables VI, VII, VIII, IX.

$C_\phi$				$\bar{C}_{\phi\phi'}$		
$uj$	$ur$	$sj$	$sr$	$\eta_u\eta_u$	$\eta_u\eta_s$	$\eta_s\eta_s$
$-1$	$-\frac{1}{2}$	$-1$	$-\frac{1}{2}$	$-\frac{1}{2}$	$1$	$-\frac{1}{2}$

TABLE VI: The coefficients  $C_\phi$  and  $\bar{C}_{\phi\phi'}$  in  $\text{PQ}\chi\text{PT}$ , which are all the same for the strangeness changing axial form factors. The  $C_\phi$  and  $\bar{C}_{\phi\phi'}$  coefficients are categorized as in Table II.

$E_\phi$							$\bar{E}_{\phi\phi'}$		
$\eta_u$	$\eta_s$	$us$	$uj$	$ur$	$sj$	$sr$	$\eta_u\eta_u$	$\eta_u\eta_s$	$\eta_s\eta_s$
$N\Lambda$	$-\frac{10}{9}$	0	$-\frac{10}{18}$	$-\frac{10}{9}$	$-\frac{10}{18}$	0	0	0	0
$\Lambda\Xi$	$-\frac{10}{27}$	0	$-\frac{20}{27}$	$-\frac{20}{27}$	$-\frac{10}{27}$	0	0	0	0
$N\Sigma$	$\frac{10}{81}$	0	$\frac{5}{81}$	$\frac{10}{81}$	$\frac{5}{81}$	0	0	0	0
$\Sigma\Xi$	$-\frac{10}{81}$	$-\frac{10}{81}$	$-\frac{40}{81}$	$-\frac{20}{81}$	$-\frac{10}{81}$	$-\frac{20}{81}$	$-\frac{10}{81}$	$-\frac{20}{81}$	$\frac{40}{81}$

TABLE VII: The coefficients  $E_\phi$  and  $\bar{E}_{\phi\phi'}$  in  $\text{PQ}\chi\text{PT}$  for the strangeness changing axial form factors. The  $E_\phi$  and  $\bar{E}_{\phi\phi'}$  coefficients are categorized as in Table II.

Finally, the non-analytic functions  $\mathcal{L}$ 's,  $\mathcal{J}$ 's,  $\mathcal{K}$ 's,  $\mathcal{R}$ 's,  $\mathcal{T}$ 's and  $\mathcal{S}$ 's in above equations are defined in section III B. Employing the same argument as one did in deriving the isospin changing pseudoscalar form factors, one arrives at a similar expression for the strangeness changing pseudoscalar form factor

$$G_{P,B'B}(q^2) = (m_B + m_{B'})^2 \left( \frac{f_K/f}{q^2 - m_K^2} G_{A,B'B}(0) \sqrt{Z_K} - \frac{1}{3} \langle r_{B'B}^2 \rangle \right), \quad (53)$$

where in this NLO expression, the axial charge  $G_{A,B'B}(0)$ , kaon mass  $m_K$  and kaon decay constant  $f_K$  are taken to be their physical values and  $Z_K$  is the kaon wavefunction renormalization which is shown in the Appendix. In fitting lattice data to Eq. (53), one would thus use the lattice measured values for  $G_{A,B'B}(0)$ ,  $m_K$  and  $f_K$ . The final term in the pseudoscalar form factor is  $\langle r_{B'B}^2 \rangle$ , which is the strangeness changing axial radius. As has been shown in section III B, the simple structure of the pseudoscalar form factor at NLO in both  $\chi\text{PT}$  and  $\text{PQ}\chi\text{PT}$  allows one to perform an approximate check of the Goldberger-Treiman relation. Here the residue of the pseudoscalar form factor at the kaon pole is proportional to the kaon-baryon-baryon coupling  $G_{KB'B}$  thus the pseudoscalar form factor provides an indirect and simple method to investigate the Goldberger-Treiman relation on the lattice.

$A_\phi$				$\bar{A}_{\phi\phi'}$	
$\eta_u$	$\eta_s$	$us$	$uj$	$\eta_u\eta_u$	$\eta_u\eta_s$
$N\Lambda$	$2D + 2F$	0	$-\frac{2}{3}D + 2F$	$\frac{16}{3}D$	0
$\Lambda\Xi$	$-\frac{2}{3}D + \frac{2}{3}F$	$\frac{2}{9}D + \frac{2}{3}F$	$\frac{4}{9}D - \frac{4}{3}F$	$\frac{20}{9}D - 4F$	$\frac{16}{9}D - \frac{8}{3}F$
$N\Sigma$	$\frac{2}{9}D + \frac{10}{9}F$	0	$\frac{2}{9}D + \frac{2}{9}F$	$\frac{16}{9}F$	$-\frac{4}{9}D + \frac{4}{3}F$
$\Sigma\Xi$	$-\frac{2}{9}D + \frac{2}{9}F$	$-\frac{2}{9}D + \frac{2}{9}F$	$\frac{4}{3}D + \frac{20}{9}F$	$\frac{4}{3}D + \frac{4}{9}F$	$\frac{4}{9}D + \frac{4}{9}F$
<hr/>				<hr/>	
	$ur$	$sj$	$sr$	$\eta_s\eta_s$	
$N\Lambda$	$\frac{8}{3}D$	0	0	0	
$\Lambda\Xi$	$\frac{10}{9}D - 2F$	$\frac{4}{9}D + \frac{4}{3}F$	$\frac{2}{9}D + \frac{2}{3}F$	$\frac{4}{9}D + \frac{4}{3}F$	
$N\Sigma$	$\frac{8}{9}F$	0	0	0	
$\Sigma\Xi$	$\frac{2}{3}D + \frac{2}{9}F$	$\frac{4}{3}D + \frac{4}{9}F$	$\frac{2}{3}D + \frac{2}{9}F$	$\frac{4}{9}D + \frac{4}{9}F$	

TABLE VIII: The coefficients  $A_\phi$  and  $\bar{A}_{\phi\phi'}$  in PQ $\chi$ PT for the strangeness changing axial form factors. The  $A_\phi$  and  $\bar{A}_{\phi\phi'}$  coefficients are categorized as in Table II.

$Y_\phi$			$\bar{Y}_{\phi\phi'}$
$\eta_u$	$\eta_s$		$\eta_u\eta_u$
$N\Lambda$	$\frac{1}{9}D^3 + 5D^2F - 9DF^2 + 3F^3$	0	$-\frac{4}{3}D^3 + 2D^2F + 12DF^2 - 18F^3$
$\Lambda\Xi$	$-\frac{5}{3}D^3 + \frac{11}{3}D^2F - 5DF^2 + 3F^3$	$-\frac{5}{9}D^3 - D^2F + DF^2 - 3F^3$	$\frac{4}{3}D^3 - \frac{22}{3}D^2F + 12DF^2 - 6F^3$
$N\Sigma$	$-\frac{1}{9}D^3 - D^2F + DF^2 + F^3$	0	$2D^2F - 8DF^2 + 6F^3$
$\Sigma\Xi$	$-\frac{1}{3}D^3 + \frac{7}{3}D^2F - DF^2 - F^3$	$-\frac{1}{3}D^3 + \frac{7}{3}D^2F - DF^2 - F^3$	$2D^2F - 2F^3$
<hr/>			$\eta_u\eta_s$
$N\Lambda$	$-\frac{25}{9}D^3 + 7D^2F - 3DF^2 - 3F^3$	$\frac{20}{9}D^3 - 4D^2F + 12DF^2 - 12F^3$	$\frac{1}{3}D^3 + D^2F - 3DF^2 - 9F^3$
$\Lambda\Xi$	$\frac{8}{9}D^3 + \frac{16}{3}D^2F - 8DF^2$	$-\frac{2}{3}D^3 - \frac{22}{3}D^2F + 14DF^2 - 6F^3$	$-\frac{1}{3}D^3 - \frac{7}{3}D^2F + 15DF^2 - 15F^3$
$N\Sigma$	$\frac{1}{9}D^3 - \frac{1}{3}D^2F + 3DF^2 - F^3$	$\frac{4}{9}D^3 + \frac{4}{3}D^2F - 4DF^2 + 4F^3$	$-D^3 + 5D^2F - 7DF^2 + 3F^3$
$\Sigma\Xi$	$-\frac{2}{3}D^3 + \frac{2}{3}D^2F - 2DF^2 + 2F^3$	$\frac{2}{3}D^3 - \frac{2}{3}D^2F + 2DF^2 - 2F^3$	$-D^3 + D^2F - 3DF^2 - 5F^3$
<hr/>			$\eta_s\eta_s$
$N\Lambda$	$\frac{10}{9}D^3 - 2D^2F + 6DF^2 - 6F^3$	0	0
$\Lambda\Xi$	$-\frac{1}{3}D^3 - \frac{11}{3}D^2F + 7DF^2 - 3F^3$	$\frac{10}{9}D^3 + \frac{10}{3}D^2F - 2DF^2 - 6F^3$	$\frac{2}{3}D^2F - 6F^3$
$N\Sigma$	$\frac{2}{9}D^3 + \frac{2}{3}D^2F - 2DF^2 + 2F^3$	0	0
$\Sigma\Xi$	$\frac{1}{3}D^3 - \frac{1}{3}D^2F + DF^2 - F^3$	$\frac{2}{3}D^3 - \frac{2}{3}D^2F + 2DF^2 - 2F^3$	$2D^2F - 2F^3$
<hr/>			
$N\Lambda$	0		
$\Lambda\Xi$	$\frac{5}{9}D^3 + \frac{5}{3}D^2F - DF^2 - 3F^3$		
$N\Sigma$	0		
$\Sigma\Xi$	$\frac{1}{3}D^3 - \frac{1}{3}D^2F + DF^2 - F^3$		

TABLE IX: The coefficients  $Y_\phi$  and  $\bar{Y}_{\phi\phi'}$  in PQ $\chi$ PT for the strangeness changing axial form factors. The  $Y_\phi$  and  $\bar{Y}_{\phi\phi'}$  coefficients are categorized as in Table II.

$u_\phi$				
	$uu$	$ss$	$jj$	$rr$
$N\Lambda$	$\frac{3}{4}b_2 + \frac{3}{4}b_5$	$\frac{3}{4}b_2$	$\frac{3}{2}b_7$	$\frac{3}{4}b_7$
$\Lambda\Xi$	$\frac{1}{2}b_1 + \frac{1}{2}b_2 + \frac{1}{4}b_3 - \frac{3}{4}b_4 + \frac{1}{2}b_5$	$\frac{1}{2}b_1 + \frac{1}{2}b_2 + \frac{1}{4}b_3 + \frac{1}{4}b_4$	$b_7 + b_6$	$\frac{1}{2}b_7 + \frac{1}{2}b_6$
$N\Sigma$	$-\frac{1}{3}b_1 - \frac{1}{12}b_2 - \frac{1}{3}b_3 + \frac{1}{3}b_4 - \frac{1}{12}b_5$	$-\frac{1}{3}b_1 - \frac{1}{12}b_2$	$-\frac{1}{6}b_7 - \frac{2}{3}b_6$	$-\frac{1}{12}b_7 - \frac{1}{3}b_6$
$\Sigma\Xi$	$-\frac{1}{6}b_1 + \frac{1}{3}b_2 - \frac{1}{12}b_3 + \frac{1}{12}b_4 + \frac{1}{6}b_5$	$-\frac{1}{6}b_1 + \frac{1}{3}b_2 - \frac{1}{12}b_3 + \frac{1}{12}b_4 + \frac{1}{6}b_5$	$\frac{2}{3}b_7 - \frac{1}{3}b_6$	$\frac{1}{3}b_7 - \frac{1}{6}b_6$

TABLE X: The coefficients  $u_\phi$  in  $\text{PQ}\chi\text{PT}$  for the strangeness changing axial form factors. The coefficients  $u_\phi$  are categorized by the mesons with mass  $m_\phi$ .

#### IV. DISCUSSION

Above we have calculated the full set of flavor-changing axial-current matrix elements of the hyperons. The expressions will be useful for the study of the chiral and momentum behavior of hyperon axial form factors using lattice QCD.

Considering the axial charges of hyperons and of their transitions, there are only two parameters which survive the chiral limit, namely  $D$  and  $F$ . As there are eight such charges, there are six relations between them. Focusing just on the isospin and strangeness transitions individually, we have four of the six relations

$$g_{NN} + g_{\Xi\Xi} - g_{\Lambda\Sigma} = 0, \quad (54)$$

$$g_{NN} - g_{\Xi\Xi} - g_{\Sigma\Sigma} = 0, \quad (55)$$

$$g_{N\Lambda} + g_{\Lambda\Xi} - 3(g_{\Sigma\Xi} - g_{N\Sigma}) = 0, \quad (56)$$

$$g_{N\Lambda} - g_{\Lambda\Xi} - g_{N\Sigma} - g_{\Sigma\Xi} = 0. \quad (57)$$

Combining isospin and strangeness transitions together, we arrive at the final two relations

$$g_{N\Lambda} + g_{\Lambda\Xi} - 3g_{\Sigma\Sigma} = 0, \quad (58)$$

$$g_{N\Lambda} - g_{\Lambda\Xi} - g_{\Lambda\Sigma} = 0. \quad (59)$$

These relations hold in  $SU(3)$   $\chi\text{PT}$ , as well as  $SU(6|3)$   $\text{PQ}\chi\text{PT}$ . Of course chiral corrections modify these relations and the “0” should be interpreted as  $\mathcal{O}(m_\phi^2/\Lambda_\chi^2)$ . The expressions derived above in section III B and III C provide these  $\mathcal{O}(m_\phi^2/\Lambda_\chi^2)$  corrections which are generally linear combinations of non-analytic loop contributions and unknown local counterterms.

The relations in Eqs. (54)–(57) actually apply not only to the axial charges, but to the respective hyperon transition matrix elements as a whole. The pseudoscalar form factors do not satisfy Eqs. (58) and (59) due to the difference in pion versus kaon poles. The axial form factors, by contrast, satisfy these latter two relations.

Apart from the axial couplings  $D$ ,  $F$ ,  $\mathcal{C}$ ,  $\mathcal{H}$ , and meson masses, the axial charges depend on six (eight) unknown parameters in  $\chi\text{PT}$  ( $\text{PQ}\chi\text{PT}$ ). This lack of predictive power historically has been overlooked by supposing, what has been termed, the formal dominance of chiral logarithms. One can do slightly better and attempt model estimation of these parameters, but the fact stands that most chiral analyses have seriously lacked the ability to make complete predictions. This is the great advantage of lattice QCD calculations, which have promise to determine the complete information about the low-energy constants.

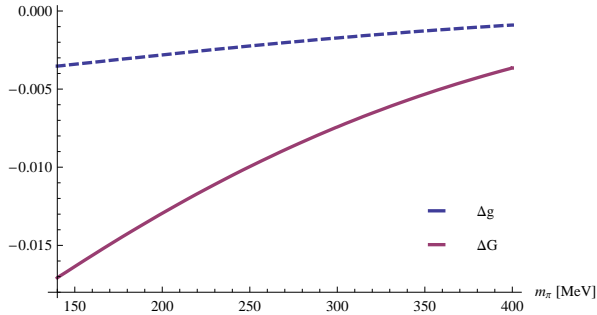


FIG. 3: Plot of  $\Delta g$  and  $\Delta G$  as a function of the pion mass  $m_\pi$ .

Despite the absence of knowledge concerning the eight coupling constants in the NLO current Eq. (26), we can make two non-trivial predictions at next-to-leading order by eliminating the local terms. The leading local terms are cancelled in the relations Eqs. (54)–(59). Combinations of these relations can be used to eliminate the next-to-leading order local terms. While there are seven contributing terms, only five of them,  $b_1, \dots, b_5$  contribute to the relations. Thus there must exist at least one combination of Eqs. (54)–(59) that is independent of the  $b_i$ . Rather fortuitously there are two such non-trivial combinations of axial charges which are independent of these couplings, *viz.*

$$\Delta g \equiv 2g_{NN} - g_{N\Lambda} - g_{N\Sigma} - g_{\Lambda\Sigma} - g_{\Sigma\Sigma} + 2g_{\Sigma\Xi}, \quad (60)$$

$$\Delta G \equiv 2g_{NN} + 2g_{\Xi\Xi} - 2g_{\Lambda\Sigma} + g_{N\Sigma} + g_{\Lambda\Xi} + g_{\Sigma\Xi} - g_{N\Lambda}. \quad (61)$$

These relations are independent of NLO counterterms in both PQ $\chi$ PT and  $\chi$ PT. The expressions for  $\Delta g$  and  $\Delta G$  in  $\chi$ PT are<sup>3</sup>

$$(4\pi f)^2 \Delta g = \frac{2}{3} \left( D^3 + 5D^2F - 6DF^2 - 6F^3 \right) \mathcal{G}[\mathcal{L}] - \mathcal{C}^2 \left[ \frac{10}{81} \mathcal{H} + \frac{1}{6} (D + F) \right] \mathcal{G}[\mathcal{J}] - \frac{2}{9} \mathcal{C}^2 (D - F) \mathcal{G}[\mathcal{K}], \quad (62)$$

$$(4\pi f)^2 \Delta G = \frac{4}{3} D (D^2 - 6F^2) \mathcal{G}[\mathcal{L}] - \frac{1}{3} D \mathcal{C}^2 \mathcal{G}[\mathcal{J}] + \frac{4}{3} F \mathcal{C}^2 \mathcal{G}[\mathcal{K}], \quad (63)$$

where the Gell-Mann Okubo linear combination functional is defined by

$$\mathcal{G}[A] = A_\pi - 4A_K + 3A_\eta, \quad (64)$$

for any function  $A_\phi = A(m_\phi, \Delta, \mu)$ . The quantities  $\Delta g$  and  $\Delta G$  allow one to test chiral logarithms directly. Accordingly these relations only superficially have scale dependence,

<sup>3</sup> Partially quenched expressions can be obtained from Eqs. (62) and (63) under the replacements:  $\mathcal{G}[\mathcal{L}] \rightarrow \mathcal{G}^{PQ}[\mathcal{L}, \mathcal{R}]$ ,  $\mathcal{G}[\mathcal{K}] \rightarrow \mathcal{G}^{PQ}[\mathcal{L}, \mathcal{S}]$ , and  $\mathcal{G}[\mathcal{J}] \rightarrow \mathcal{G}^{PQ}[\mathcal{L}, \mathcal{T}]$ . The partially quenched functional is given by

$$\mathcal{G}^{PQ}[A, B] = 2A_\pi - 4A_K + 2A_{\eta_s} + 2B_{\eta_u \eta_u} - 4B_{\eta_u \eta_s} + 2B_{\eta_s \eta_s},$$

for any function  $A_\phi = A(m_\phi, \Delta, \mu)$  and hairpin function  $B_{\eta_\phi \eta_{\phi'}} = B(\eta_\phi \eta_{\phi'}, \Delta, \mu)$ . There is no scale dependence in  $\mathcal{G}^{PQ}[A, B]$ .

and upon the limit of  $SU(3)_V$  symmetry, they vanish. With these symmetry breaking relations, we have separated out the short distance physics and hence isolated long-distance chiral corrections. To obtain values for  $\Delta g$  and  $\Delta G$ , as well as the curve shown in Fig. 3, we have fixed the strange quark mass at its physical value, and used the  $SU(6)$  values for the axial couplings:  $D = 3/4$ ,  $F = 2/3D$ ,  $\mathcal{C} = -2D$ , and  $\mathcal{H} = -3D$ . In particular, we find  $\Delta g = -0.0035$  and  $\Delta G = -0.017$  at physical pion mass  $m_\pi = 140$  MeV.

Four further non-trivial relations, analogous to  $\Delta g$  and  $\Delta G$  above, exist when one includes charges arising from the strangeness axial current  $\bar{s}\gamma_\mu\gamma_5s$ . These matrix elements have been determined at zero momentum transfer in  $\text{PQ}\chi\text{PT}$  [33]. Determination of these charges requires the calculation of disconnected operator contractions on the lattice. As such contributions are notoriously difficult to determine, we leave it to future work to deduce the remaining symmetry breaking relations.

### Acknowledgments

We thank G. Colangelo for discussions. This work is supported in part by the U.S. Dept. of Energy, Grant Nos. DE-FG02-05ER41368-0 and DE-FG02-93ER40762 (B.C.T.) and by the Schweizerischer Nationalfonds (F.-J.J.).

## WAVE FUNCTION RENORMALIZATION

In this appendix, we list the necessary wave function renormalization and meson  $Z$ -factors appearing in the calculations. For the baryons, we have [39]

$$Z_B = 1 - \frac{1}{16\pi^2 f^2} \left( \sum_\phi \mathcal{A}_\phi \mathcal{L}_\phi + \sum_{\phi, \phi'} \mathcal{A}_{\phi\phi'} \mathcal{R}_{\phi\phi'} + \mathcal{C}^2 \left( \sum_\phi \mathcal{B}_\phi \mathcal{J}_\phi + \sum_{\phi, \phi'} \mathcal{B}_{\phi\phi'} \mathcal{T}_{\phi\phi'} \right) \right) \quad (65)$$

where the coefficient  $\mathcal{A}_\phi$ ,  $\bar{\mathcal{A}}_{\phi, \phi'}$ ,  $\mathcal{B}_\phi$ ,  $\bar{\mathcal{B}}_{\phi\phi'}$  and are given in Tables XI, XII. For the mesons, one has

$$Z_\varphi = 1 + \frac{2}{3} \left( \frac{1}{16\pi^2 f^2} \sum_\phi C_\phi \mathcal{L}(m_\phi, \mu) \right) - \frac{2}{\lambda} \left( (2m_{jj}^2 + m_{rr}^2) \alpha_4 + w_\varphi \alpha_5 \right), \quad (66)$$

where  $\alpha_4$  and  $\alpha_5$  are the low energy constants that appear in  $\mathcal{L}^4$  in the meson sector. Further, for  $\varphi = \pi$ ,  $w_\pi = m_{uu}^2$  and one uses Table I for  $C_\phi$  while for  $\varphi = K$ ,  $w_K = m_{us}^2$  and one uses Table VI for  $C_\phi$ . Finally the non-analytic functions  $\mathcal{J}$ 's and  $\mathcal{L}$ 's are given in section III B.

---

[1] T. DeGrand and C. DeTar, *Lattice Methods for Quantum Chromodynamics* (World Scientific, 2006).

[2] C. W. Bernard and M. F. L. Golterman, Phys. Rev. **D46**, 853-857 (1992), hep-lat/9204007.

[3] C. W. Bernard and M. F. L. Golterman, Phys. Rev. **D49**, 486-494 (1994), hep-lat/9306005.

[4] S. R. Sharpe and N. Shores, Phys. Rev. **D62**, 094503 (2000), hep-lat/0006017.

[5] S. R. Sharpe and N. Shores, Phys. Rev. **D64**, 114510 (2001), hep-lat/0108003.

$\mathcal{A}_\phi$			$\bar{\mathcal{A}}_{\phi\phi'}$
$\eta_u$	$\eta_s$	$us$	$\eta_u\eta_u$
$N$	$-4D(D - 3F)$	0	$3(D - 3F)^2$
$\Lambda$	$-\frac{2}{3}D^2 + 8DF - 6F^3$	0	$\frac{4}{3}(2D - 3F)^2$
$\Sigma$	$2(3F^2 - D^2)$	0	$12F^2$
$\Xi$	0	$2(3F^2 - D^2)$	$3(D - F)^2$
$uj$			$\eta_u\eta_s$
$N$	$10D^2 - 12DF + 18F^2$	$5D^2 - 6DF + 9F^2$	0
$\Lambda$	$\frac{28}{3}D^2 - 16DF + 12F^2$	$\frac{14}{3}D^2 - 8DF + 6F^2$	$-\frac{4}{3}(2D^2 + 3DF - 9F^2)$
$\Sigma$	$4D^2 + 12F^2$	$2D^2 + 6F^2$	$12F(F - D)$
$\Xi$	$6(D - F)^2$	$3(D - F)^2$	$12F(F - D)$
$sr$			$\eta_s\eta_s$
$N$	0		0
$\Lambda$	$\frac{1}{3}(D + 3F)^2$		$\frac{1}{3}(D + 3F)^2$
$\Sigma$	$3(D - F)^2$		$3(D - F)^2$
$\Xi$	$2(D^2 + 3F^2)$		$12F^2$

TABLE XI: The coefficients  $\mathcal{A}_\phi$  and  $\bar{\mathcal{A}}_{\phi\phi'}$  in PQ $\chi$ PT for the wave function renormalization. The  $\mathcal{A}_\phi$  and  $\bar{\mathcal{A}}_{\phi\phi'}$  coefficients are categorized as in Table II.

$\mathcal{B}_\phi$							$\bar{\mathcal{B}}_{\phi\phi'}$		
$\eta_u$	$\eta_s$	$us$	$uj$	$ur$	$sj$	$sr$	$\eta_u\eta_u$	$\eta_u\eta_s$	$\eta_s\eta_s$
$N$	2	0	0	2	1	0	0	0	0
$\Lambda$	1	0	1	2	1	0	0	0	0
$\Sigma$	$\frac{1}{3}$	0	$\frac{5}{3}$	$\frac{2}{3}$	$\frac{1}{3}$	$\frac{4}{3}$	$\frac{2}{3}$	$-\frac{4}{3}$	$\frac{2}{3}$
$\Xi$	0	$\frac{1}{3}$	$\frac{5}{3}$	$\frac{4}{3}$	$\frac{2}{3}$	$\frac{2}{3}$	$\frac{2}{3}$	$-\frac{4}{3}$	$\frac{2}{3}$

TABLE XII: The coefficients  $\mathcal{B}_\phi$  and  $\bar{\mathcal{B}}_{\phi\phi'}$  in PQ $\chi$ PT for the wave function renormalization. The  $\mathcal{B}_\phi$  and  $\bar{\mathcal{B}}_{\phi\phi'}$  coefficients are categorized as in Table II.

- [6] S. R. Sharpe and R. L. Singleton, Phys. Rev. **D58**, 074501 (1998), hep-lat/9804028.
- [7] W. Lee and S. R. Sharpe, Phys. Rev. **D60**, 114503 (1999), hep-lat/9905023.
- [8] R. G. Edwards et al., Phys. Rev. Lett **96**, 052001 (2006), hep-lat/0510062.
- [9] QCDSF Collaboration (A. Ali Khan et al.), Phys. Rev **D74**, 094508 (2006), hep-lat/0603028.
- [10] S. R. Beane and M. Savage, Nucl. Phys. **A709**, 319-344 (2002), hep-lat/0203003.
- [11] T. R. Hemmert, M. Procura and W. Weise, Phys. Rev. **D68**, 075009 (2003), hep-lat/0303002.
- [12] M. Procura, B. U. Musch, T. R. Hemmert and W. Weise, Phys. Rev. **D75**, 014503 (2007), hep-lat/0610105.
- [13] S. R. Beane and M. J. Savage, Phys. Rev. **D68**, 114502 (2003), hep-lat/0306036.
- [14] F. J. Jiang, arXiv:hep-lat/0703012.
- [15] S. R. Beane and M. J. Savage, Phys. Rev. **D70**, 074029 (2004), hep-ph/0404131.
- [16] W. Detmold and M. J. Savage, Phys. Lett. **B599**, 32-42 (2004), hep-lat/0407008.

- [17] B. Smigelski and J. Wasem, Phys. Rev. **D76**, 074503 (2007), arXiv: 0706.3731.
- [18] E. Jenkins and A. V. Manohar, Phys. Lett. **B255**, 558 (1991).
- [19] E. Jenkins and A. V. Manohar, Phys. Lett. **B259**, 353 (1991).
- [20] E. Jenkins, Nucl. Phys. **B375**, 561 (1992).
- [21] R.P. Springer, hep-ph/9508324
- [22] M.J. Savage and J. Walden, Phys. Rev. **D55**, 5376 (1997), hep-ph/9611210.
- [23] B. Borasoy and B. R. Holstein, Eur. Phys. J. **C** 6 (1999) 85, hep-ph/9805430.
- [24] A. Abd El-Hady, J. Tandean and G. Valencia, Nucl. Phys. **A651**, 71-89 (1999), hep-ph/9808322.
- [25] R.P. Springer, Phys. Lett **B461**, 167-174 (1999)
- [26] A. Abd El-Hady and J. Tandean, Phys. Rev. **D61**, 114014 (2000), hep-ph/9908498.
- [27] S. R. Beane, P. F. Bedaque, A. Parreno, M. J. Savage, Nucl. Phys. **A747**, 55-74 (2005), nucl-th/0311027.
- [28] A. Gasparyan, J. Haidenbauer, C. Hanhart and J. Speth, Phys. Rev. **C69**, 034006 (2004), hep-ph/0311116.
- [29] F. Hinterberger and A. Sibirtsev, Eur. Phys. J. **A21**, 313-321 (2004), nucl-ex/0402021.
- [30] S. R. Beane et al., hep-lat/0612026.
- [31] H.-W. Lin, arXiv:0707.3844 [hep-lat].
- [32] H.-W. Lin and K. Orginos, arXiv:0712.1214 [hep-lat].
- [33] W. Detmold and C. J. David Lin, Phys. Rev. **D71**, 054510 (2005), hep-lat/0501007.
- [34] O. Bar, C. Bernard, G. Rupak and N. Shores, Phys. Rev. D **72**, 054502 (2005) [arXiv:hep-lat/0503009].
- [35] B. C. Tiburzi, Phys. Rev. D **72**, 094501 (2005) [arXiv:hep-lat/0508019].
- [36] J. W. Chen, D. O'Connell and A. Walker-Loud, arXiv:0706.0035 [hep-lat].
- [37] J. N. Labrenz and S. R. Sharpe, Phys. Rev. **D54**, 4595 (1996), hep-lat/9605034.
- [38] M. J. Savage, Nucl. Phys. **A700**, 359 (2002), nucl-th/0107038.
- [39] J.-W. Chen and M. J. Savage, Phys. Rev. **D65**, 094001 (2002), hep-lat/0111050.
- [40] V. Bernard, H. W. Fearing, T. R. Hemmert and U. G. Meissner, Nucl. Phys. A **635**, 121 (1998) [Erratum-ibid. A **642**, 563 (1998 NUPHA,A642,563-563.1998)], arXiv:hep-ph/9801297.
- [41] B. Borasoy, Phys. Rev. **D59**, 054021 (1999), hep-ph/9811411.
- [42] V. Bernard, L. Elouadrhiri and U. G. Meissner, J. Phys. G **28**, R1 (2002), arXiv:hep-ph/0107088.
- [43] M. R. Schindler, T. Fuchs, J. Gegelia and S. Scherer, Phys. Rev. C **75**, 025202 (2007), arXiv:nucl-th/0611083.
- [44] Ph. Hagler *et al.* [LHPC Collaborations], arXiv:0705.4295 [hep-lat].
- [45] C. Alexandrou, G. Koutsou, T. Leontiou, J. W. Negele and A. Tsapalis, arXiv:0706.3011 [hep-lat].
- [46] M. Kim and S. Kim, Phys. Rev **D58**, 074509 (1998), hep-lat/9608091.
- [47] J. Kambor and M. Mojzis, JHEP 9904:031 (1999), hep-ph/9901235.
- [48] W. Detmold, W. Melnitchouk and A. W. Thomas, Phys. Rev. **D66**, 054501 (2002), hep-lat/0206001.
- [49] S.-L. Zhu, S. Puglia and M. J. Ramsey-Musolf, Phys. Rev. **D63**, 034002 (2001), hep-ph/0008140.
- [50] V. Bernard and Ulf-G. Meissner, Phy. Lett. **B639**, 278-282 (2006), hep-lat/0605010.
- [51] B. C. Tiburzi, Phys. Rev. **D71**, 054504 (2005), hep-lat/0412025.
- [52] S. L. Adler and Y. Dothan, Phys. Rev. **151**, 1267 (1966).

[53] B. C. Tiburzi, Phys. Lett. **B617**, 40 (2005), hep-lat/0504002.